Supplementary Information for:

Designing Anisotropic Cyanometallate Coordination Polymers with Unidirectional Thermal Expanison (TE): 2D Zero TE and 1D Colossal Positive TE

Ania S. Sergeenko, Jeffrey S. Ovens, Daniel B. Leznoff*

Department of Chemistry, Simon Fraser University, 8888 University Drive, Burnaby, British Columbia, V5A 1S6, Canada

E-mail: dleznoff@sfu.ca

1 Experimental

1.1 General Procedures and Physical Measurements

All reactions were performed in air at room temperature. $Cu(H_2O)_2[PtBr_2(CN)_4]$ (**1**), $Cu(H_2O)_2[PtCl_2(CN)_4]$ (**2**), $Cu[PtBr_2(CN)_4]$ (**3**) and $Cu[PtCl_2(CN)_4]$ (**4**) were synthesized using literature procedures.[1] Infrared spectra were measured on a Thermo Nicolet Nexus 670 FT-IR spectrometer equipped with a Pike MIRacle attenuated total reflection (ATR) sampling accessory. Raman spectra were measured using a Renishaw inVia Raman microscope with a 514 nm laser at 5-10% intensity for 15 to 60 seconds or 785 nm laser at 10-50% intensity for 5 to 20 seconds. A Linkam THMS600 temperature controlled stage was added for the collection of variable temperature Raman spectra. Differential scanning calorimetry was performed at a rate of 10˚C/minute from 0 to -90˚C by David Ester on a DSC Q2000 V24.9.

1.2 X-Ray Crystallographic Analysis

Samples were mounted on MiTeGen sample holders using paratone oil. All crystallographic data was collected on a Bruker SMART ApexII Duo CCD diffractometer with TRIUMPH graphite-monochromated Mo Kα (λ = 0.71073 Å) radiation for single crystal data collection and a Cu Kα (λ = 1.54184 Å) Incoatec microsource using ω and ϕ scans for powder data collection. The temperature was controlled using an Oxford Cryosystems Cryostream with a wait time of twenty minutes for equilibration after each change in temperature. All single crystal diffraction data was processed and initial solutions found with the Bruker ApexII software suite. Subsequent refinements were performed in SHELXle.[2]

Crystallographic information for **1-LT** can be found in Table S1. **1-LT** was solved as a two-component pseudo-merohedral twin. It was suggested by SHELXle that the space group for **1-LT** is P2/m, not $P2_1/m$, but attempts at solution using P2/m resulted in unstable refinements.

Three hydrogen atoms in **1-LT** were found and placed; attempts to place the remaining hydrogen atom resulted in unstable refinements.

Due to the moderate quality of single crystal data from these compounds, all variable temperature experiments were collected on powder samples. All powder X-ray diffraction (PXRD) data was processed using the Bruker ApexII software suite and analyzed using Topas Academic software.[3] PXRD patterns for **1-LT**, **1-HT** and **3** can be found in Figure S4. PXRD patterns for **2-LT**, **2-HT** and **4** can be found in Figure S9. To collect variable temperature data, powder X-ray diffraction data were collected every 30 K upon cooling and heating, resulting in data collection at intervals of 15 K with no evidence of hysteresis. Rietveld refinements were performed on each of the diffraction patterns**.** Since the crystallographic axes of **1-LT**, **2-LT**, **3** and **4** did not correspond to the axes containing the Pt-CN-Cu sheets or the inter-sheet distance as in **1-HT** and **2-HT**, they were re-defined by determining the d-spacing between two points of interest so as to be able to compare thermal expansion parameters. Errors were propagated using standard methods. Crystallographic information for both the original and transformed unit cells of **1**-**4** can be found in Tables S3 to S10. Figures were made using ORTEP-3, POV-Ray, SigmaPlot, and GIMP 2.[4–7]

1.3 Thermal Expansion

All thermal expansion coefficients were determined using the slopes of linear ranges and can be found in Table 1. Due to the symmetry of **1** and **2** the distances between all four Pt-CN-Cu linkages are equivalent; inequivalencies in axes are the result of C-Pt-C angles deviating slightly from square planarity, therefore thermal expansion parameters were reported using the original definition of axes.

The unit cell parameters for **1-LT** between 105 K and 195 K can be found in Table S3. Upon transformation of the unit cell parameters of **1-LT** to match the definition of the cell for **1-HT**, all unit cell parameters for **1** were combined into Table S5 and have been plotted in Figures 5 and S8. Thermal expansion coefficients for **1** were calculated using data from the linear portion of the curve (from 105 to 150 K). After 150 K the rate of change becomes non-linear until the compound undergoes the phase change.

The unit cell parameters for **2-LT** between 105 and 165 K can be found in Table S4. After transformation of the unit cell parameters of **2-LT** to match the definition of the cell for **2-HT** all unit cell parameters for **2** were combined into Table S6 and have been plotted in Figures S10 and S11. Due to the ease of dehydration under anhydrous conditions and at temperatures above 255 K, for the **2-HT** the thermal expansion coefficients were determined using data from the linear range of 180 K to 255 K. Upon partial dehydration a global shrinking effect can be seen as the aqua ligands begin to depart and chloride ligands begin to bridge sheets. The thermal expansion within the 2-D nets of both **2-LT and 2-HT** are so small that their absolute values are difficult to measure within the limitations of our instrument, resulting in errors larger than the measured value. Additionally, the error in **2-LT** is increased as a result of redefining the axes to match those of **2-HT**. While the directionality of the thermal expansion coefficients in **2** within the 2-D sheet are difficult to elucidate, by looking at the peak positions in the PXRD patterns one can see for the *001* plane (along the OXO view direction) there is a slight shift from $2\theta \sim 12.08$ to 12.03 upon cooling, corresponding to negative thermal expansion.

Graphs for the pre-transformed cell parameters with temperature for **3** and **4** can be found in Fig. S12 and S13 respectively. The errors calculated for the transformed unit cell parameters in **4**

are higher than those for the original cell parameters due in large part to error propagation of the beta angle; the errors are larger than those in **3** due to slightly lower relative intensity of the PXRD patterns.

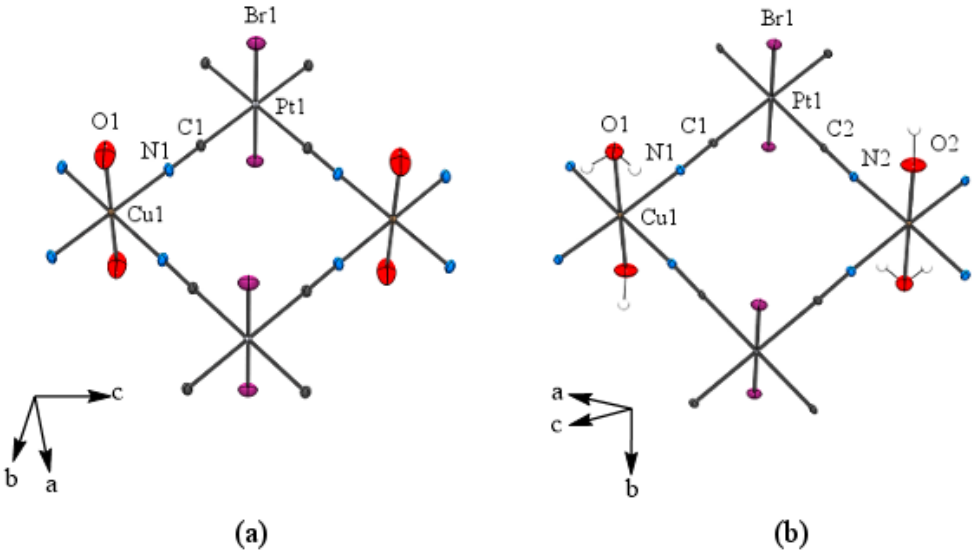

Figure S1: Crystal structures of one square grid of (a) **1-HT**; (b) **1-LT**.

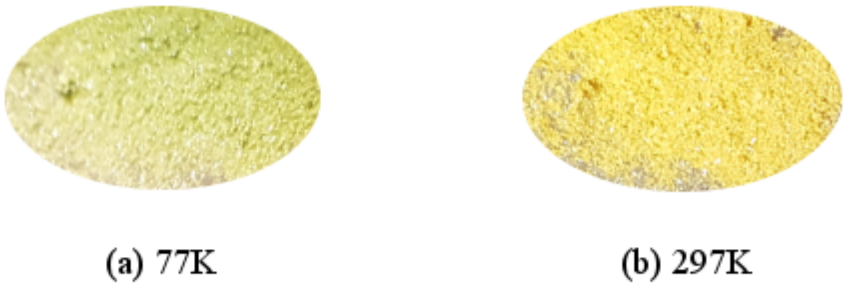

Figure S2: Thermochromism of **1**: (a) **1-LT**; (b) **1-HT**

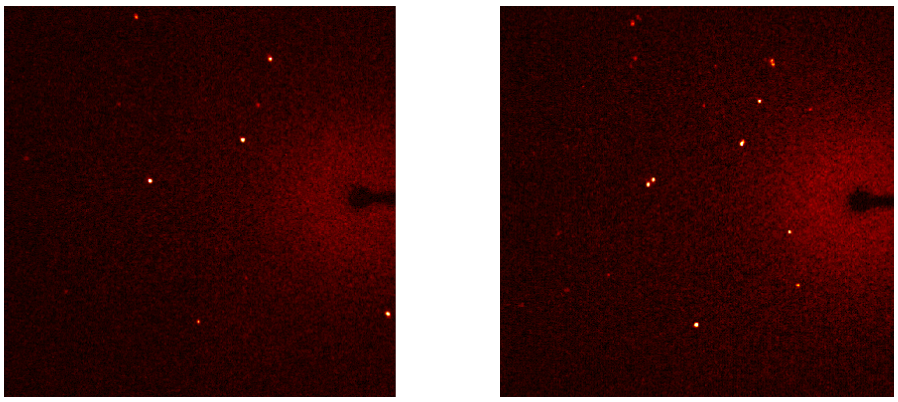

(a) **HT-1** (above 210K) (b) **LT-1** (below 210K)

Figure S3: Two frames from single crystal X-ray diffraction of **1**: (a) **1-HT**; (b) **1-LT**.

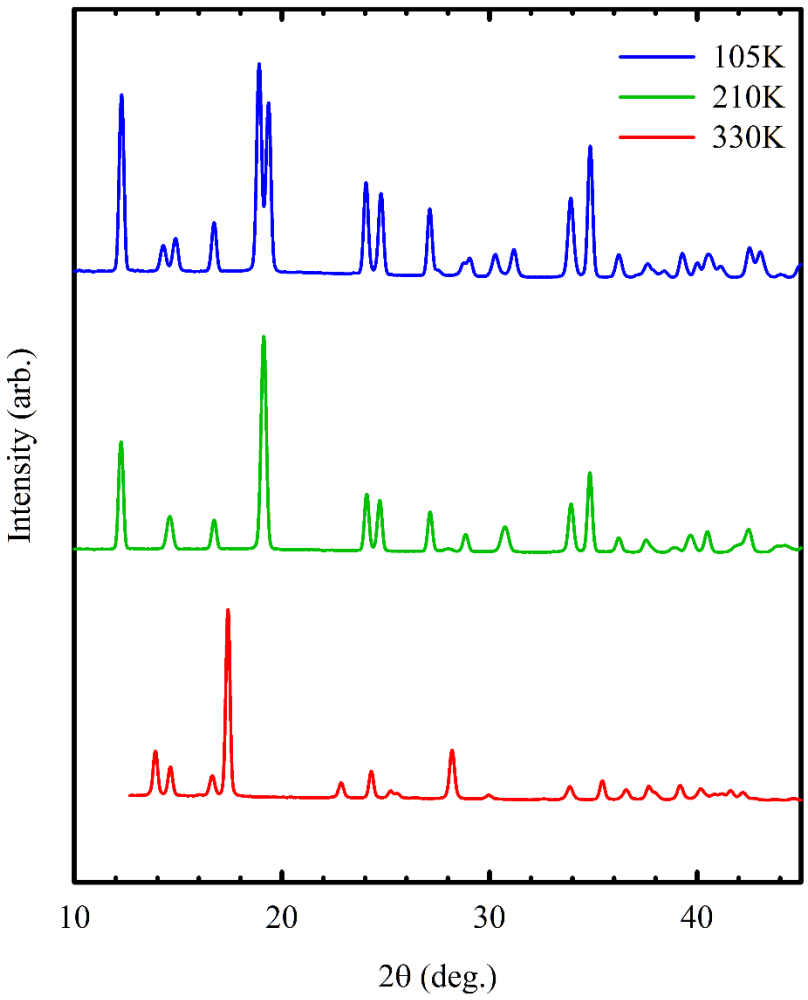

Figure S4: Powder X-ray diffractograms of **1-LT** (blue; 105 K), **1-HT** (green; 210 K) and **3** (red; 330 K).

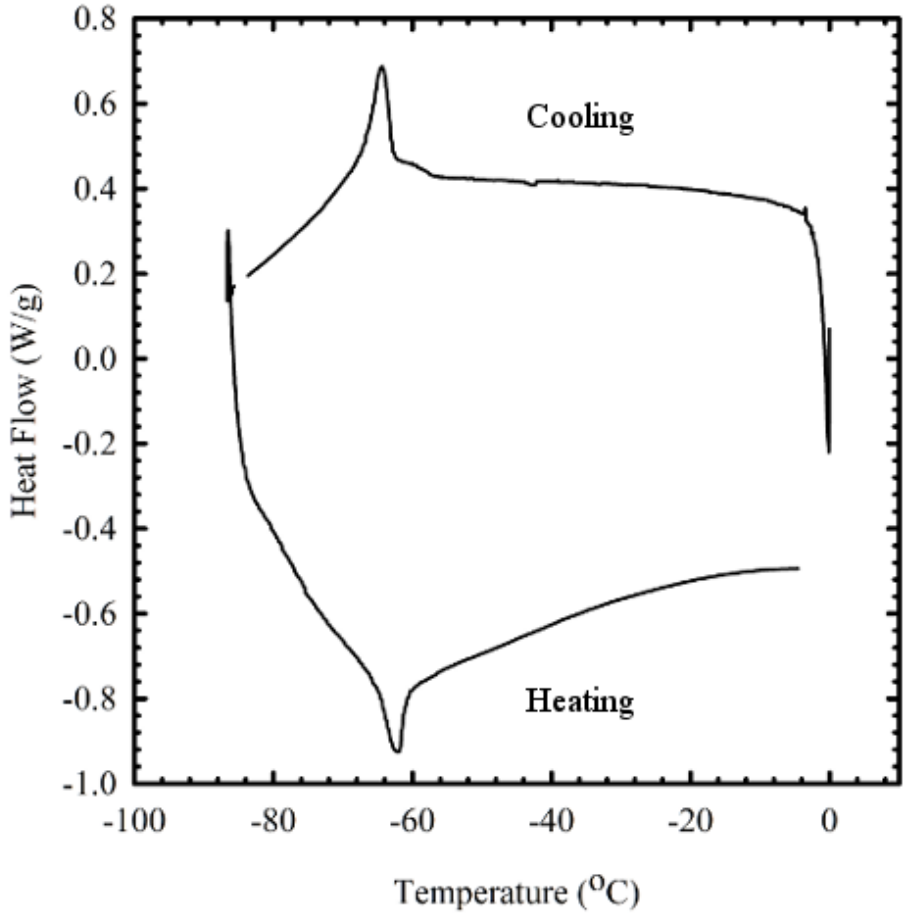

Figure S5: Phase transition of $Cu(H_2O)_2[PtBr_2(CN)_4]$ (**1**) monitored by differential scanning calorimetry.

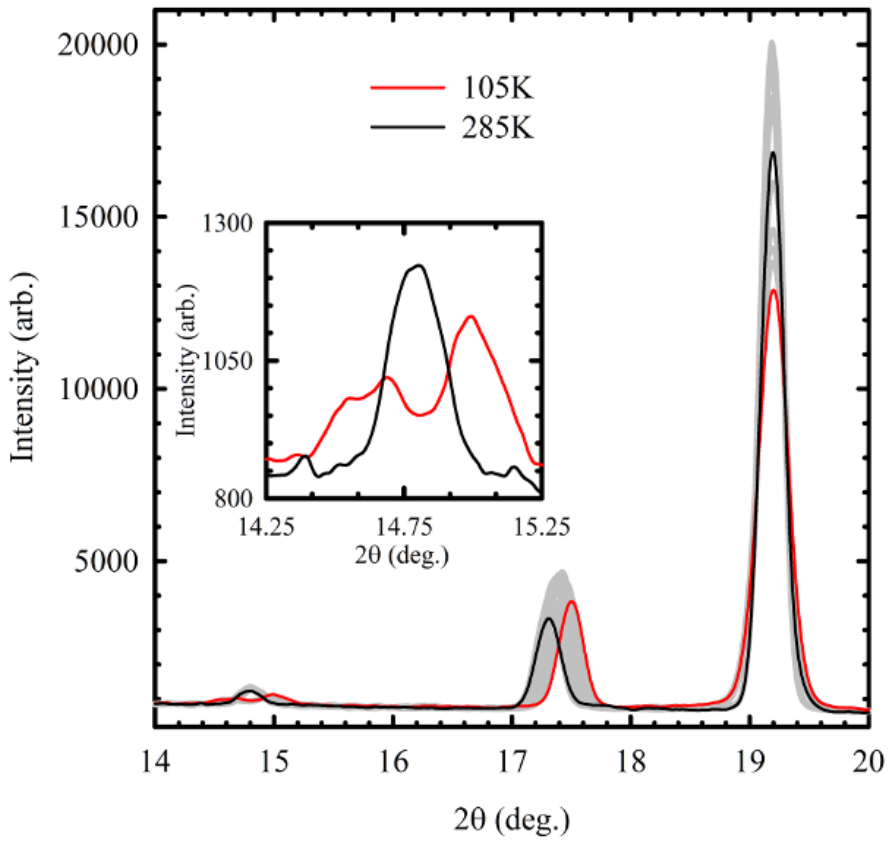

Figure S6: Powder X-ray diffraction patterns of $Cu(H_2O)_2[PtCl_2(CN)_4]$ (**2**) from 105 K to 285 K in 15 K intervals. Inset: Splitting of the peak corresponding to the *110* plane at 105 K.

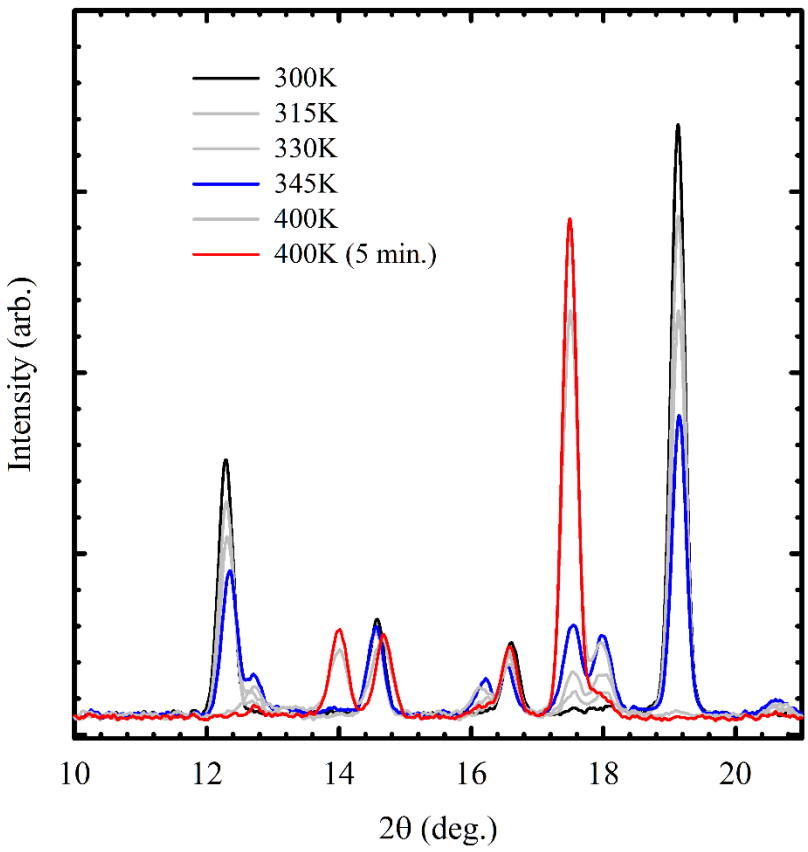

Figure S7: Powder X-ray diffractograms of $Cu(H_2O)_2[PtBr_2(CN)_4]$ (**1-HT**, black; 300 K) as it converts first to an intermediate, $Cu(H_2O)[PtBr_2(CN)_4]\cdot H_2O$ (blue; 345 K), and then $Cu[PtBr_2(CN)_4]$ (**3**, red; 400 K).

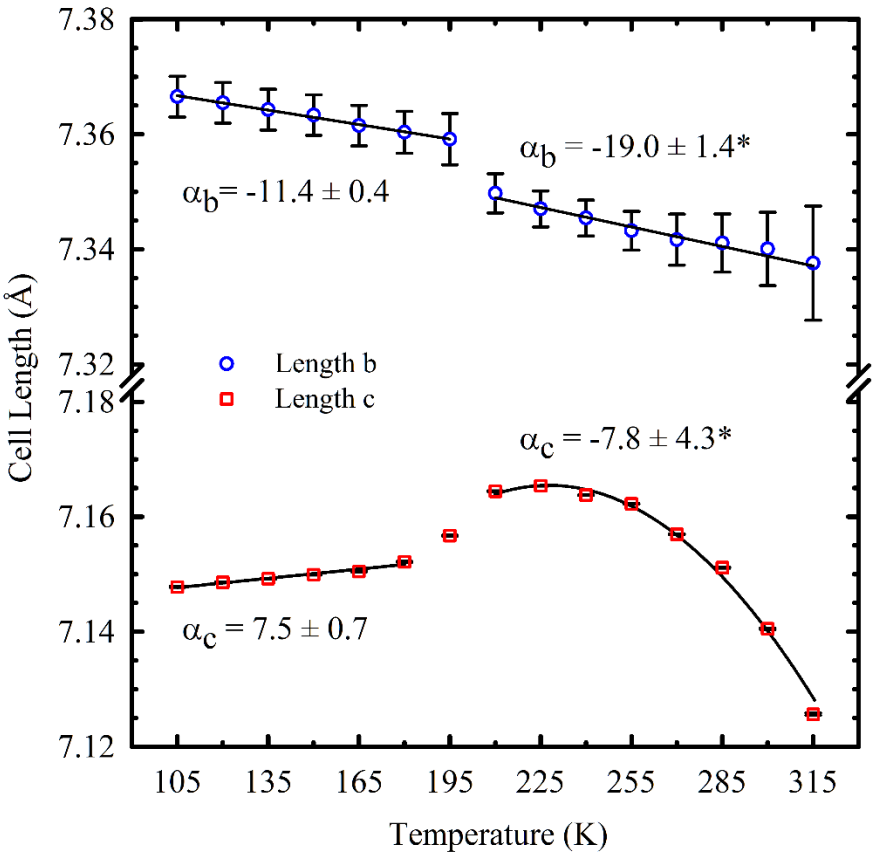

Figure S8: Zoomed view of the unit cell parameters as a function of temperature for $Cu(H_2O)_2[PtBr_2(CN)_4]$ (**1**).

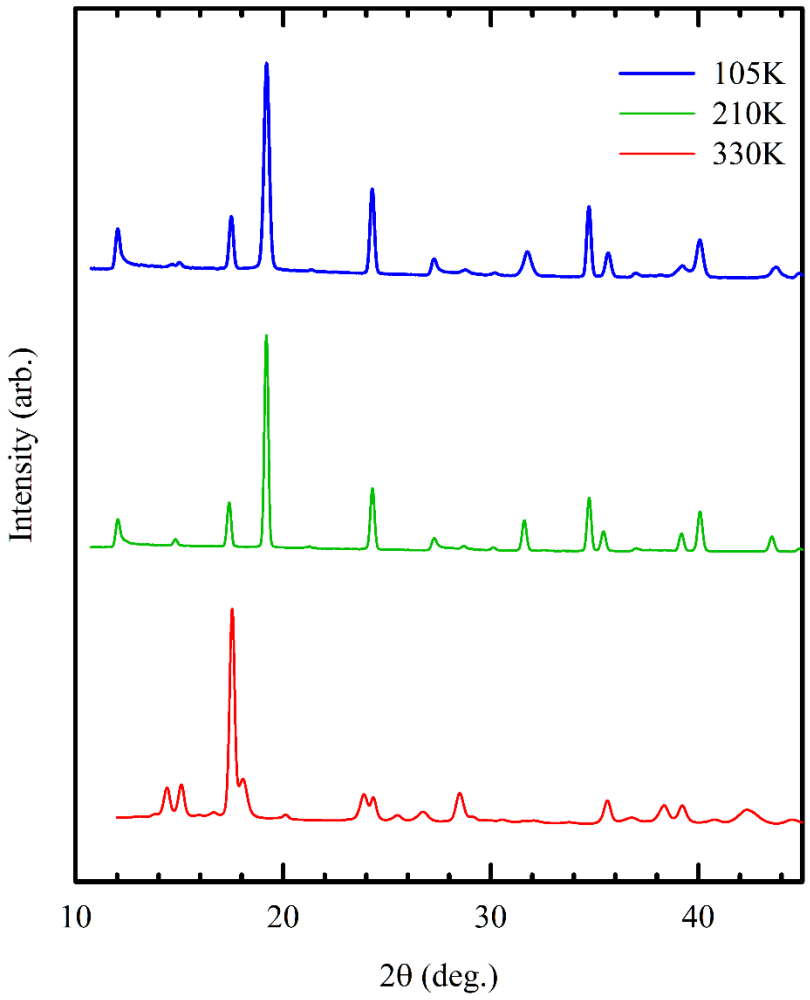

Figure S9: Powder X-ray diffractograms of **2-LT** (blue; 105 K), **2-HT** (green; 210 K) and **4** (red; 330 K).

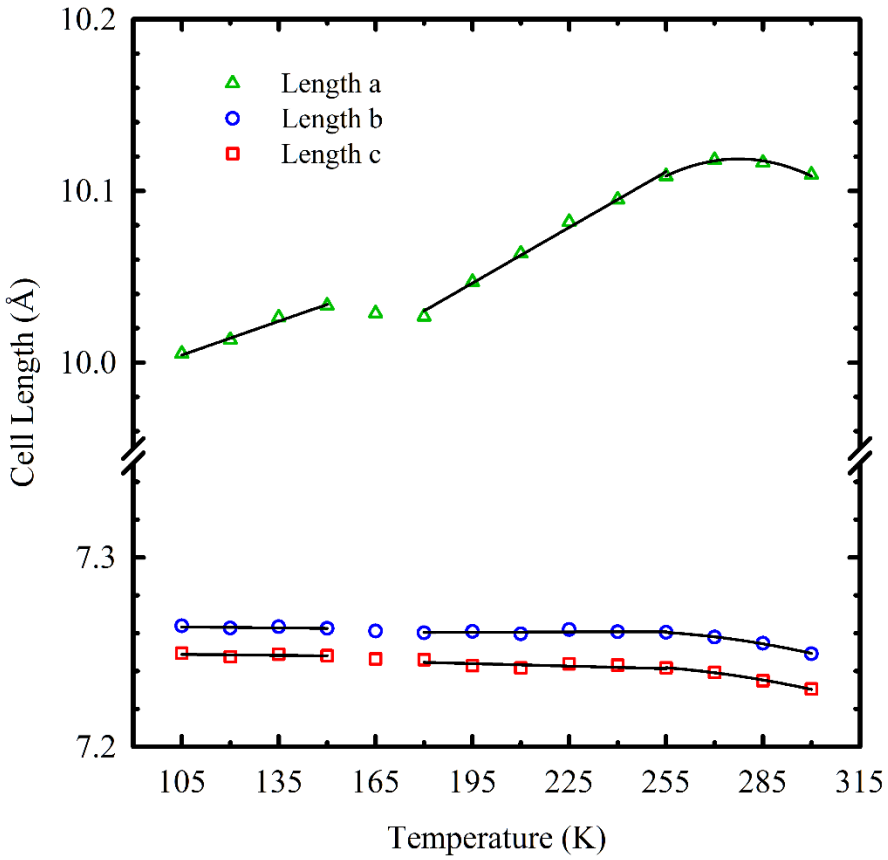

Figure S10: Unit cell parameters as a function of temperature for $Cu(H_2O)_2[PtCl_2(CN)_4]$ (**2**). Error bars are within the points.

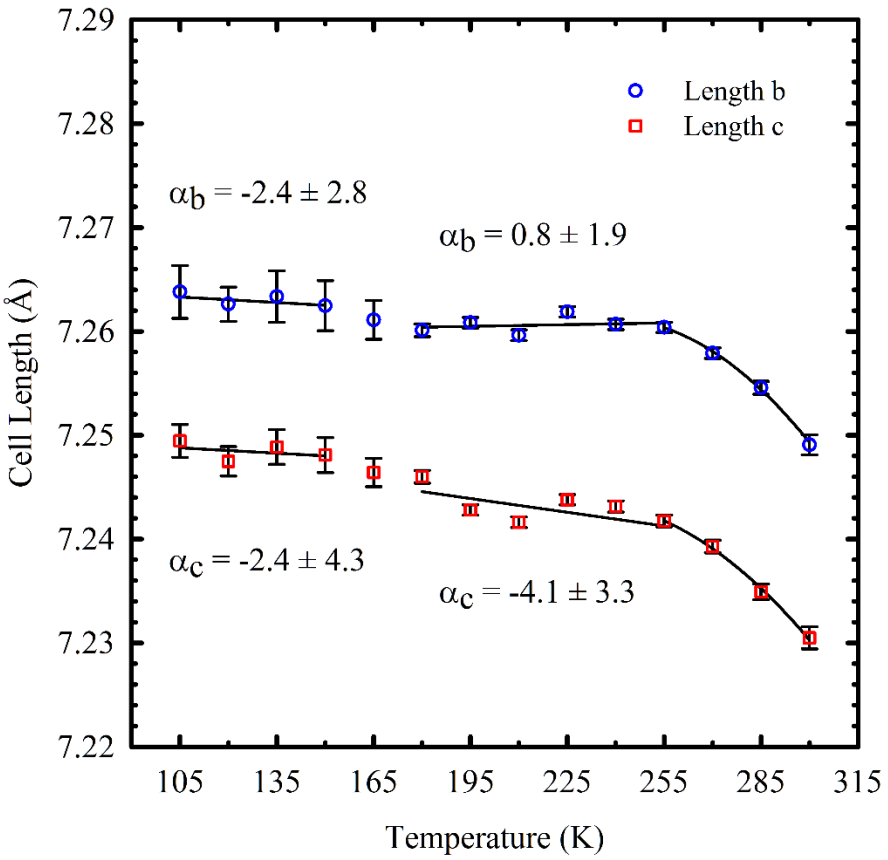

Figure S11: Zoomed view of the unit cell parameters as a function of temperature for $Cu(H_2O)_2[PtCl_2(CN)_4]$ (**2**). Error bars are within the points.

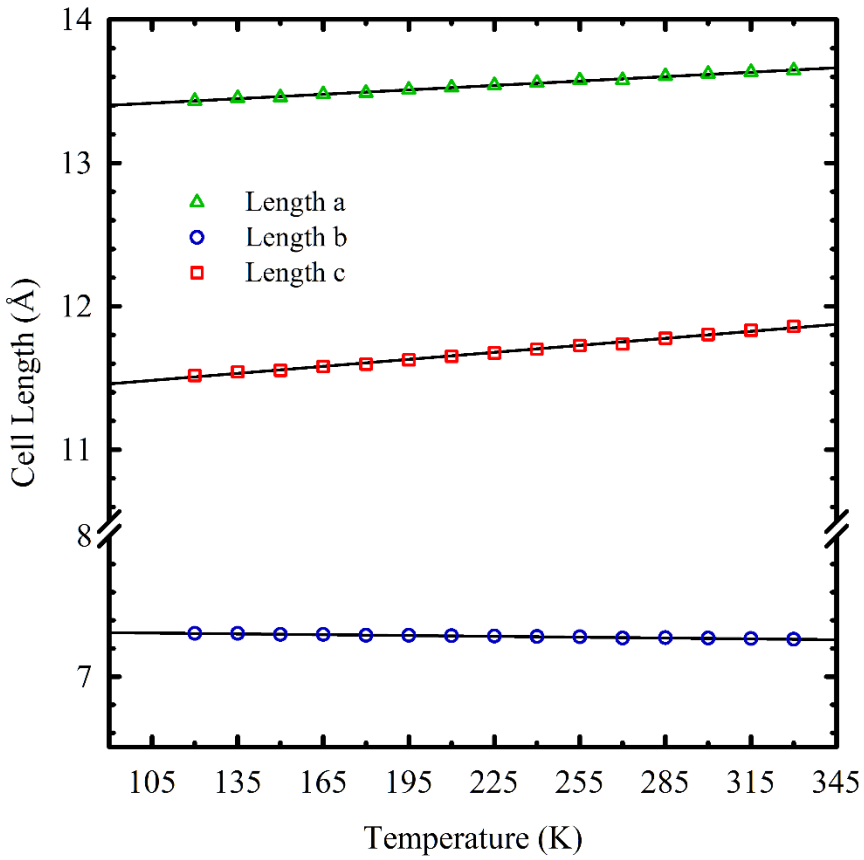

Figure S12: Change in pre-transformed cell lengths of **3** with temperature. Error bars are within the points.

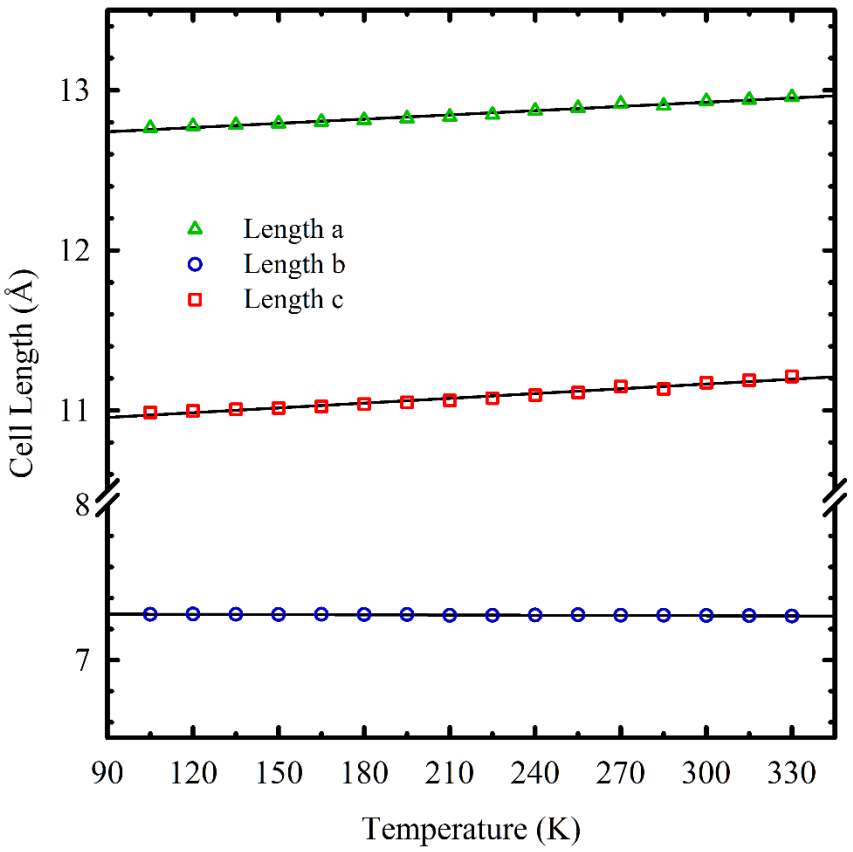

Figure S13: Change in pre-transformed cell lengths of **4** with temperature. Error bars are within the points.

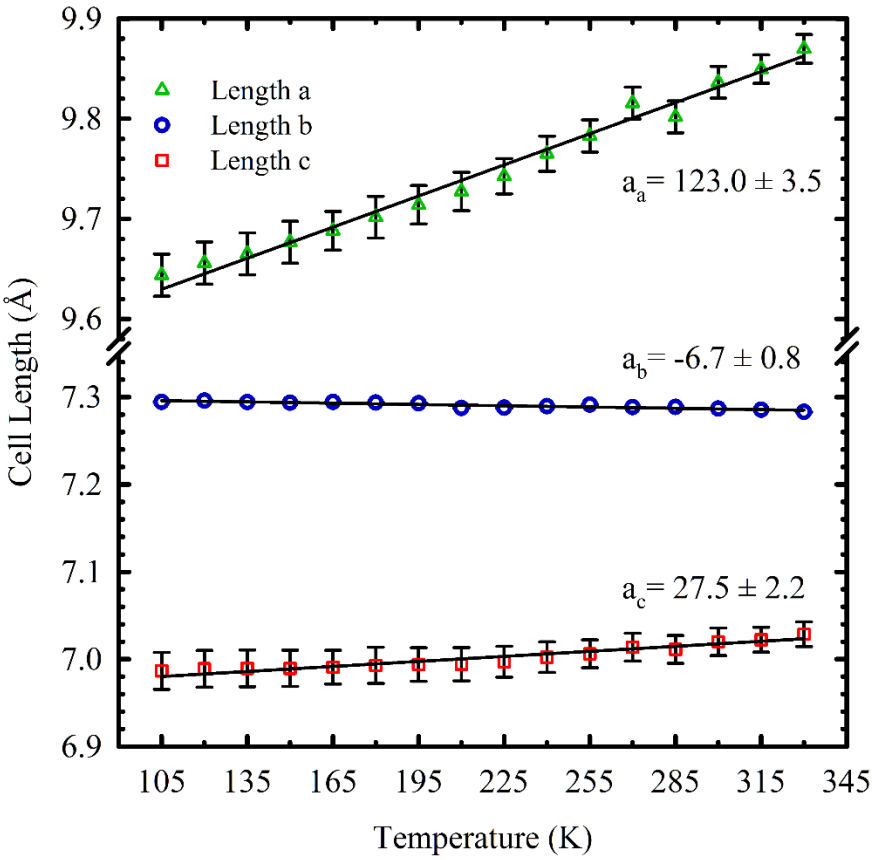

Figure S14: Change in transformed cell lengths of **4** with temperature.

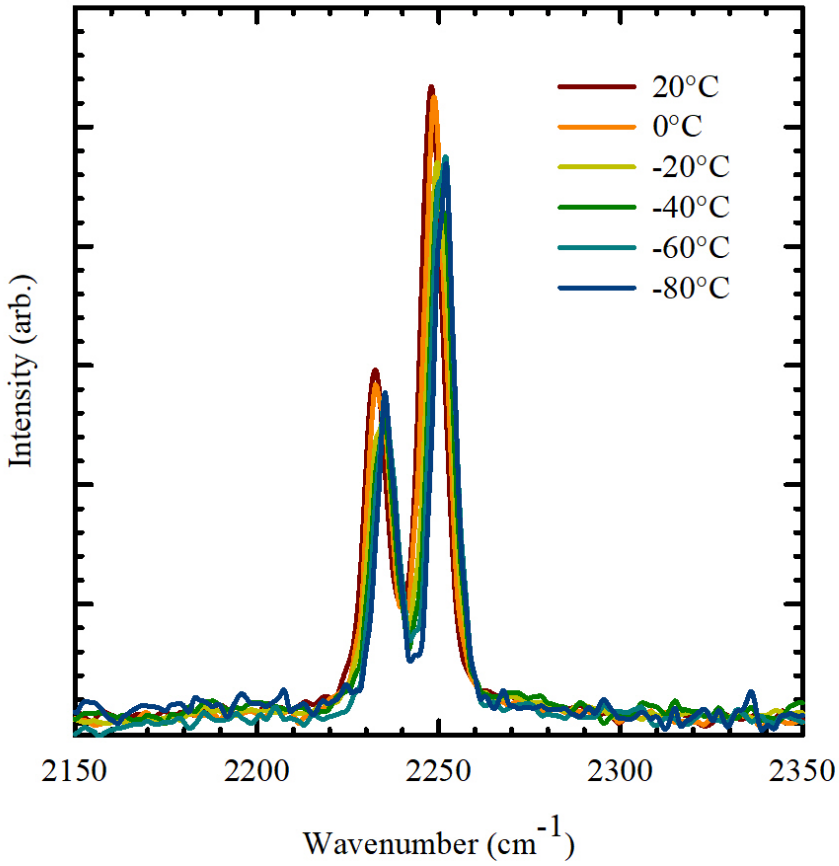

Figure S15: Variable temperature Raman spectra from 20°C to -80°C showing the phase change at -60°C (210K).

Table S1. Crystallographic information for **1-LT**

	1-LT
empirical formula	$C_4H_4N_4O_2Br_2CuPt$
formula weight (g mol^{-1})	558.53
crystal dimensions (mm)	0.048, 0.103, 0.145
crystal system	monoclinic
space group	$P2_1/m$
a (Å)	6.3039(6)
b (Å)	14.2946(13)
c (Å)	6.5640(6)
α (deg)	90
β (deg)	110.207(2)
γ (deg)	90
V ($Å^3$)	555.09(9)
Z	2
T (K)	135(2)
ρ_{calcd} (g cm^{-3})	3.336
μ (mm)	21.680
$2\theta_{max}$ (deg.)	33.24
total/unique reflections	2208/1665
obsd reflns [$I_0 \geq 2\sigma(I_0)$]	1665
R_1, wR_2 [$I_0 \geq 2\sigma(I_0)$][a]	0.0141, 0.0309
GOF	1.074
largest difference peak/hole (e^-/ $Å^3$)	1.160/ -0.985
CCDC no.	1580083

Table S2: Selected interatomic distances in $Cu(H_2O)_2[PtBr_2(CN)_4]$ (**1-LT**)

	Distance (Å)
Pt(1)-C(1)	2.009(3)
Pt(1)-C(2)	2.005(3)
C(1)-N(1)	1.140(4)
C(2)-N(2)	1.144(4)
Pt(1)-Br(1)	2.4781(3)
Cu(1)-N(1)	1.988(3)
Cu(1)-N(2)	1.985(3)
Cu(1)-O(1)	2.467(3)
Cu(1)-O(2)	2.309(3)
O(1)-H(1)	0.92(2)
O(2)-H(2)	0.88(2)
Br(1)- Br(1)’	3.6996(8)
Br(1)-Br(1)’’	3.7048(8)
Br(1)-O(1)’	3.5175(6)
O(1)-O(2)’	2.978(5)

Table S3: Cell Lengths resulting from Rietveld Analysis of the low temperature phase $Cu(H_2O)_2[PtBr_2(CN)_4]$ (**1-LT**)

Temp. (K)	A axis (Å)	+/-	B axis (Å)	+/-	C axis (Å)	+/-	Beta (˚)	+/-	Volume ($Å^3$)	+/-
105	6.29711	0.00025	14.29557	0.00058	6.55675	0.00025	110.1002	0.0026	554.294	0.039
120	6.30110	0.00025	14.29717	0.00058	6.55731	0.00025	110.1392	0.0026	554.616	0.039
135	6.30568	0.00025	14.29843	0.00057	6.55727	0.00024	110.1793	0.0026	554.922	0.038
150	6.31069	0.00025	14.29986	0.00058	6.55679	0.00025	110.2163	0.0026	555.246	0.039
165	6.31660	0.00025	14.30098	0.00057	6.55499	0.00024	110.2599	0.0026	555.501	0.038
180	6.32453	0.00026	14.30430	0.00059	6.55180	0.00026	110.2994	0.0027	555.915	0.040
195	6.33580	0.00030	14.31342	0.00067	6.54237	0.00031	110.3193	0.0033	556.387	0.047

Table S4: Cell Lengths resulting from Rietveld Analysis of the low temperature phase $Cu(H_2O)_2[PtCl_2(CN)_4]$ (**2-LT**)

Temp. (K)	A axis (Å)	+/-	B axis (Å)	+/-	C axis (Å)	+/-	Beta (˚)	+/-	Volume ($Å^3$)	+/-
105	6.1520	0.0012	14.5091	0.0033	6.2211	0.0010	108.054	0.012	527.95	0.18
120	6.1557	0.0012	14.5044	0.0033	6.2225	0.0010	108.103	0.012	528.07	0.18
135	6.1630	0.0012	14.5080	0.0032	6.2265	0.0010	108.164	0.012	528.99	0.18
150	6.1700	0.0013	14.5079	0.0032	6.2260	0.0011	108.209	0.012	529.40	0.19
165	6.1912	0.0099	14.5004	0.0036	6.19734	0.0008	108.213	0.011	528.49	0.17

Table S5: Combined cell lengths for both **1-LT** and **1-HT**

Temp. (K)	A axis (Å)	+/-	B axis (Å)	+/-	C axis (Å)	+/-
105	10.5368	0.0036	7.3665	0.0036	7.147785	0.000073
120	10.5430	0.0035	7.3655	0.0035	7.148585	0.000073
135	10.5492	0.0035	7.3643	0.0035	7.149215	0.000071
150	10.5553	0.0035	7.3633	0.0035	7.149930	0.000073
165	10.5614	0.0035	7.3615	0.0035	7.150490	0.000071
180	10.5677	0.0036	7.3603	0.0036	7.152150	0.000074
195	10.5704	0.0045	7.3591	0.0045	7.156710	0.000084
210	10.5241	0.0034	7.3497	0.0034	7.164430	0.000064
225	10.5321	0.0031	7.3470	0.0031	7.165375	0.000055
240	10.5455	0.0031	7.3454	0.0031	7.163750	0.000056
255	10.5595	0.0034	7.3432	0.0034	7.162245	0.000065
270	10.5757	0.0044	7.3417	0.0044	7.156945	0.000088
285	10.5913	0.0051	7.3411	0.0051	7.151160	0.000100
300	10.6058	0.0064	7.3401	0.0064	7.140500	0.000125

Table S6: Combined cell lengths for both **2-LT** and **2-HT**

Temp. (K)	A axis (Å)	+/-	B axis (Å)	+/-	C axis (Å)	+/-
105	10.014	0.018	7.268	0.018	7.25455	0.00041
120	10.021	0.018	7.267	0.018	7.25220	0.00041
135	10.034	0.018	7.268	0.018	7.25400	0.00040
150	10.042	0.018	7.268	0.018	7.25395	0.00040
165	10.036	0.017	7.263	0.017	7.25020	0.00045
180	10.02809	0.00066	7.25734	0.00068	7.24907	0.00080
195	10.04796	0.00062	7.25730	0.00065	7.24582	0.00075
210	10.06442	0.00061	7.25600	0.00063	7.24461	0.00073
225	10.08286	0.00061	7.25869	0.00062	7.24709	0.00071
240	10.09595	0.00063	7.25823	0.00062	7.24624	0.00071
255	10.10950	0.00065	7.25750	0.00062	7.24518	0.00071
270	10.11785	0.00072	7.25502	0.00064	7.24165	0.00072
285	10.11621	0.00080	7.25191	0.00069	7.23747	0.00077
300	10.1045	0.00100	7.24639	0.00087	7.23058	0.00093

Table S7: Cell Lengths resulting from Rietveld Analysis of $Cu[PtBr_2(CN)_4]$ (**3**)

Temp. (K)	A axis (Å)	+/-	B axis (Å)	+/-	C axis (Å)	+/-	Beta (˚)	+/-	Volume ($Å^3$)	+/-	R_{wp}
120	13.4329	0.0012	7.30700	0.00052	11.5178	0.0010	67.9453	0.0052	1047.80	0.16	2.700
135	13.4524	0.0011	7.30671	0.00049	11.54227	0.00097	67.8839	0.0050	1051.05	0.15	2.674
150	13.45781	0.00072	7.29970	0.00030	11.55358	0.00064	67.8124	0.0037	1050.957	0.096	2.039
165	13.47876	0.00068	7.29910	0.00029	11.58075	0.00061	67.7487	0.0036	1054.502	0.092	2.015
180	13.48871	0.00074	7.29332	0.00033	11.59740	0.00062	67.6841	0.0036	1055.473	0.098	2.040
195	13.51129	0.00069	7.29344	0.00031	11.62701	0.00058	67.6117	0.0035	1059.405	0.092	1.964
210	13.52614	0.00070	7.29000	0.00032	11.65039	0.00060	67.5465	0.0036	1061.703	0.095	1.965
225	13.54229	0.00084	7.28798	0.00039	11.67409	0.00071	67.4660	0.0042	1064.22	0.11	2.266
240	13.55879	0.00072	7.28511	0.00033	11.70140	0.00063	67.4063	0.0037	1067.125	0.098	2.024
255	13.57543	0.00069	7.28232	0.00032	11.72724	0.00061	67.3405	0.0035	1069.872	0.095	1.926
270	13.5772	0.0013	7.27310	0.00072	11.7375	0.00012	67.2552	0.0043	1068.92	0.18	2.581
285	13.60561	0.00072	7.27588	0.00033	11.77670	0.00066	67.2020	0.0036	1074.73	0.10	1.925
300	13.62076	0.00074	7.27352	0.00033	11.80276	0.00070	67.1360	0.0037	1077.44	0.10	2.061
315	13.63400	0.00069	7.26967	0.00032	11.83351	0.00067	67.0774	0.0035	1080.255	0.099	1.837
330	13.64477	0.00071	7.26436	0.00033	11.86028	0.00070	67.0081	0.0036	1082.21	0.10	1.851

Table S8: Transformed Unit Cell Parameters for $Cu[PtBr_2(CN)_4]$ (**3**)

Temp. (K)	A axis (Å)	+/-	B axis (Å)	+/-	C axis (Å)	+/-
120	10.3597	0.0064	7.30700	0.00016	7.0163	0.0064
135	10.3815	0.0062	7.30671	0.00015	7.0228	0.0061
150	10.3927	0.0045	7.29970	0.00010	7.0207	0.0045
165	10.4164	0.0044	7.29910	0.00010	7.0281	0.0044
180	10.4313	0.0044	7.29332	0.00010	7.0293	0.0044
195	10.4572	0.0042	7.29344	0.00010	7.0369	0.0042
210	10.4769	0.0044	7.29000	0.00010	7.0412	0.0044
225	10.4982	0.0051	7.28798	0.00010	7.0446	0.0051
240	10.5199	0.0044	7.28511	0.00009	7.0508	0.0044
255	10.5414	0.0042	7.28232	0.00009	7.0561	0.0042
270	10.5515	0.0051	7.27310	0.00019	7.0513	0.0051
285	10.5827	0.0043	7.27588	0.00010	7.0645	0.0043
300	10.6037	0.0044	7.27352	0.00010	7.0694	0.0044
315	10.6254	0.0041	7.26967	0.00010	7.0753	0.0041
330	10.6451	0.0042	7.26436	0.00010	7.0785	0.0042

Table S9: Cell Lengths resulting from Rietveld Analysis of $Cu[PtCl_2(CN)_4]$ (**4**)

Temp. (K)	A axis (Å)	+/-	B axis (Å)	+/-	C axis (Å)	+/-	Beta (˚)	+/-	Volume ($Å^3$)	+/-	R_{wp}
105	12.7643	0.0031	7.2943	0.0021	10.9866	0.0025	71.632	0.014	970.81	0.43	8.615
120	12.7768	0.0031	7.2959	0.0021	10.9964	0.0025	71.582	0.014	972.57	0.43	8.627
135	12.7829	0.0031	7.2942	0.0021	11.0061	0.0025	71.534	0.014	973.38	0.43	8.875
150	12.7925	0.0035	7.2936	0.0023	11.0151	0.0025	71.469	0.014	974.46	0.47	9.024
165	12.8029	0.0033	7.2944	0.0021	11.0250	0.0024	71.415	0.013	975.93	0.44	8.827
180	12.8134	0.0036	7.2937	0.0022	11.0394	0.0025	71.355	0.014	977.56	0.47	9.146
195	12.8240	0.0035	7.2929	0.0020	11.0499	0.0024	71.293	0.013	978.85	0.44	8.958
210	12.8340	0.0037	7.2875	0.0020	11.0621	0.0025	71.222	0.013	979.54	0.45	9.248
225	12.8476	0.0033	7.2877	0.0018	11.0769	0.0023	71.159	0.012	981.55	0.41	9.022
240	12.8713	0.0030	7.2894	0.0016	11.0954	0.0024	71.072	0.012	984.72	0.39	8.791
255	12.8882	0.0027	7.2913	0.0014	11.1119	0.0022	71.003	0.011	987.34	0.35	8.686
285	12.9147	0.0025	7.2884	0.0013	11.1485	0.0022	70.883	0.011	991.50	0.33	8.618
270	12.9034	0.0027	7.2886	0.0014	11.1341	0.0023	70.939	0.011	989.72	0.36	8.697
300	12.9316	0.0025	7.2867	0.0013	11.1732	0.0023	70.818	0.011	994.39	0.34	8.398
315	12.9412	0.0023	7.2854	0.0012	11.1882	0.0022	70.7632	0.099	995.95	0.31	8.216
330	12.9573	0.0023	7.2830	0.0012	11.2121	0.0023	70.703	0.010	998.62	0.32	8.093

Table S10: Transformed Unit Cell Parameters for $Cu[PtCl_2(CN)_4]$ (**4**)

Temp. (K)	A axis (Å)	+/-	B axis (Å)	+/-	C axis (Å)	+/-
105	9.643845	0.021083	7.2943	0.000415	6.986603	0.021083237
120	9.655928	0.021022	7.2959	0.000415	6.989046	0.021021882
135	9.665163	0.020963	7.2942	0.000414	6.989493	0.020963284
150	9.676625	0.020885	7.2936	0.000414	6.989504	0.020884549
165	9.688115	0.019333	7.2944	0.000397	6.990913	0.019332378
180	9.701767	0.020748	7.2937	0.000413	6.992961	0.02074752
195	9.714066	0.019197	7.2929	0.000396	6.993894	0.019197067
210	9.727322	0.019119	7.2875	0.000412	6.994285	0.019119195
225	9.742633	0.017585	7.2877	0.000378	6.997169	0.017584971
240	9.765104	0.017498	7.2894	0.000394	7.002276	0.017497931
255	9.78285	0.015977	7.2913	0.000361	7.00613	0.015977024
285	9.815608	0.015869	7.2884	0.00036	7.01378	0.015868897
270	9.801816	0.015919	7.2886	0.000376	7.011231	0.015919291
300	9.836349	0.015811	7.2867	0.000375	7.019941	0.015810969
315	9.8496	0.014186	7.2854	0.000358	7.022152	0.014186237
330	9.869771	0.014281	7.283	0.000374	7.028654	0.014281323

1 A. S. Sergeenko, J. S. Ovens and D. B. Leznoff, *Inorg. Chem.*, 2017, **56**, 7870–7881.

2 C. B. Hübschle, G. M. Sheldrick and B. Dittrich, *J. Appl. Crystallogr.*, 2011, **44**, 1281–1284.

3 Coelho Software, 2012.

4 L. J. Farrugia, *J. Appl. Crystallogr.*, 2012, **45**, 849–854.

5 T. D. Fenn, D. Ringe and G. A. Petsko, *J. Appl. Crystallogr.*, 2003, **36**, 944–947.

6 Systat Software, 2013.

7 P. Mattis and S. Kimball, *URL http//www. gimp. org*, 2007, 1–706.